



# Bis-imidazoles as molecular probes for peripheral sites of the zinc endopeptidase of botulinum neurotoxin serotype A

Isidro Merino,<sup>a</sup> Jason D. Thompson,<sup>a</sup> Charles B. Millard,<sup>b</sup>  
James J. Schmidt<sup>c,\*</sup> and Yuan-Ping Pang<sup>a,\*</sup>

<sup>a</sup>Computer-Aided Molecular Design Laboratory, Mayo Clinic College of Medicine, 200 First Street SW, Rochester, MN 55905, USA

<sup>b</sup>Walter Reed Army Institute of Research, Division of Biochemistry, 503 Robert Grant Avenue, Silver Spring, MD 20910, USA

<sup>c</sup>Department of Cell Biology and Biochemistry, Integrated Toxicology Division,

United States Army Medical Research Institute of Infectious Diseases, 1425 Porter Street, Frederick, MD 21702, USA

Received 14 October 2005; revised 10 January 2006; accepted 10 January 2006

Available online 2 February 2006

**Abstract**—Botulinum neurotoxin serotype A (BoNTA) is highly toxic, and its antidote is currently unavailable. The essential light-chain subunit of BoNTA is a zinc endopeptidase that can be used as a target for developing antidotes. However, the development of high-affinity, small-molecule inhibitors of the endopeptidase is as challenging as the development of small-molecule inhibitors of protein–protein complexation. This is because the polypeptide substrate wraps around the circumference of the endopeptidase upon binding, thereby constituting an unusually large substrate–enzyme interface of 4840 Å<sup>2</sup>. To overcome the large-interface problem, we propose using the zinc-coordination and bivalence approaches to design inhibitors of BoNTA. Here we report the development of alkylene-linked bis-imidazoles that inhibit the endopeptidase in a two-site binding mode. The bis-imidazole tethered with 13 methylene groups, the most potent of the alkylene-linked dimers, showed 61% inhibition of the zinc endopeptidase of BoNTA at a concentration of 100 μM. The results demonstrate the presence of a peripheral binding site for an imidazolium group at the rim of the BoNTA active-site cleft. This peripheral site enables the use of the bivalence approach to improve our previously reported small-molecule inhibitors that were developed according to the zinc-coordination approach.

© 2006 Elsevier Ltd. All rights reserved.

## 1. Introduction

Botulinum neurotoxin serotype A (BoNTA) is a  $M_r \sim 150,000$  protein produced by the spore-forming anaerobic bacterium, *Clostridium botulinum*. The neurotoxin consists of a light chain ( $M_r \sim 50,000$ ) and a heavy chain ( $M_r \sim 100,000$ ), covalently linked by a disulfide bond. BoNTA poisoning inhibits the release of acetylcholine from presynaptic nerve terminals at neuromuscular junctions, thus causing flaccid paralysis and leading to death by respiratory arrest or prolonged mechanical ventilation with serious medical sequelae.<sup>1</sup> Nonetheless, BoNTA is used as an effective medical treatment for a variety of cholinergic nerve–muscle dysfunctions.<sup>2,3</sup> In addition to its useful medical applica-

tions, BoNTA has gained notoriety as a potential bioterror agent.<sup>4</sup> Currently there is no chemical antidote to BoNTA. Therefore, effective small-molecule inhibitors of BoNTA are highly sought after as antidotes, as well as potential medical tools for modulating the clinical use of the toxin.

The light-chain domain of BoNTA is a zinc endopeptidase (hereafter referred to as the endopeptidase) that specifically cleaves SNAP-25, a neuronal protein, that is required for acetylcholine release,<sup>5</sup> and it has been used as a target for developing small-molecule inhibitors of BoNTA.<sup>6,7</sup> However, the development of small-molecule inhibitors of the endopeptidase is as challenging as the development of small-molecule inhibitors of protein–protein complexes. This is because, upon binding, the substrate wraps around the circumference of the endopeptidase constituting an unusually large substrate–enzyme interface of 4840 Å<sup>2</sup>,<sup>8</sup> which requires unusually high-affinity small molecules to block the interface.

**Keywords:** Food poisoning; Bioterrorism; Antidotes; Protease; Zinc protein simulations; Structure-based drug design.

\* Corresponding authors. Tel.: +1 301 619 4240; fax: +1 301 619 2348 (J.J.S.); tel.: +1 507 284 7868; fax: +1 507 284 9111 (Y.-P.P.); e-mail addresses: james.schmidt@det.amedd.army.mil; pang@mayo.edu

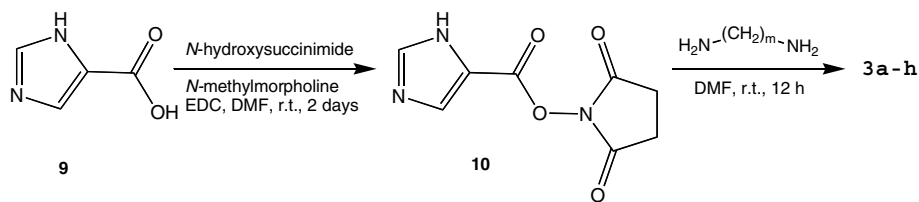
## Report Documentation Page

*Form Approved*  
*OMB No. 0704-0188*

Public reporting burden for the collection of information is estimated to average 1 hour per response, including the time for reviewing instructions, searching existing data sources, gathering and maintaining the data needed, and completing and reviewing the collection of information. Send comments regarding this burden estimate or any other aspect of this collection of information, including suggestions for reducing this burden, to Washington Headquarters Services, Directorate for Information Operations and Reports, 1215 Jefferson Davis Highway, Suite 1204, Arlington VA 22202-4302. Respondents should be aware that notwithstanding any other provision of law, no person shall be subject to a penalty for failing to comply with a collection of information if it does not display a currently valid OMB control number.

1. REPORT DATE <b>9 FEB 2006</b>	2. REPORT TYPE <b>N/A</b>	3. DATES COVERED	
4. TITLE AND SUBTITLE <b>Bis-imidazoles as molecular probes for peripheral sites of the zinc endopeptidase of botulinum neurotoxin serotype A, Bioorganic and Medicinal Chemistry 14:3584 - 3591</b>		5a. CONTRACT NUMBER	
		5b. GRANT NUMBER	
		5c. PROGRAM ELEMENT NUMBER	
6. AUTHOR(S) <b>Merino /I Thompson, JD Millard, CB Schmidt, JJ Pang, Y-P</b>		5d. PROJECT NUMBER	
		5e. TASK NUMBER	
		5f. WORK UNIT NUMBER	
7. PERFORMING ORGANIZATION NAME(S) AND ADDRESS(ES) <b>United States Army Medical Research Institute of Infectious Diseases, Fort Detrick, MD</b>		8. PERFORMING ORGANIZATION REPORT NUMBER	
9. SPONSORING/MONITORING AGENCY NAME(S) AND ADDRESS(ES)		10. SPONSOR/MONITOR'S ACRONYM(S)	
		11. SPONSOR/MONITOR'S REPORT NUMBER(S)	
12. DISTRIBUTION/AVAILABILITY STATEMENT <b>Approved for public release, distribution unlimited.</b>			
13. SUPPLEMENTARY NOTES <b>The original document contains color images.</b>			
14. ABSTRACT <b>Botulinum neurotoxin serotype A (BoNTA) is highly toxic, and its antidote is currently unavailable. The essential light-chain subunit of BoNTA is a zinc endopeptidase that can be used as a target for developing antidotes. However, the development of high-affinity, small-molecule inhibitors of the endopeptidase is as challenging as the development of small-molecule inhibitors of protein-protein complexation, This is because the polypeptide substrate wraps around the circumference of the endopeptidase upon binding, thereby constituting an unusually large substrate-enzyme interface of 4840 Å. To overcome the large interface problem, we propose using the zinc-coordination and bivalence approaches to design inhibitors of BoNTA. Here we report the development of alkylene-linked bis-imidazoles that inhibit the endopeptidase in a two-site binding mode. The bis-imidazole tethered with 13 methylene groups, the most potent of the alkylene-linked dimers, showed a 61% inhibition of the zinc endopeptidase of BoNTA at a concentration of 100 µM. The results demonstrate the presence of a peripheral binding site for an imiazolium group at the rim of the BoNTA active-site cleft. This peripheral site enables the use of the bivalence approach to improve our previously reported small-molecule inhibitors that were developed according the the zinc-coordination. approach.</b>			
15. SUBJECT TERMS			
16. SECURITY CLASSIFICATION OF:			17. LIMITATION OF ABSTRACT
a. REPORT <b>unclassified</b>	b. ABSTRACT <b>unclassified</b>	c. THIS PAGE <b>unclassified</b>	<b>SAR</b>
			18. NUMBER OF PAGES <b>9</b>
			19a. NAME OF RESPONSIBLE PERSON





Scheme 2.

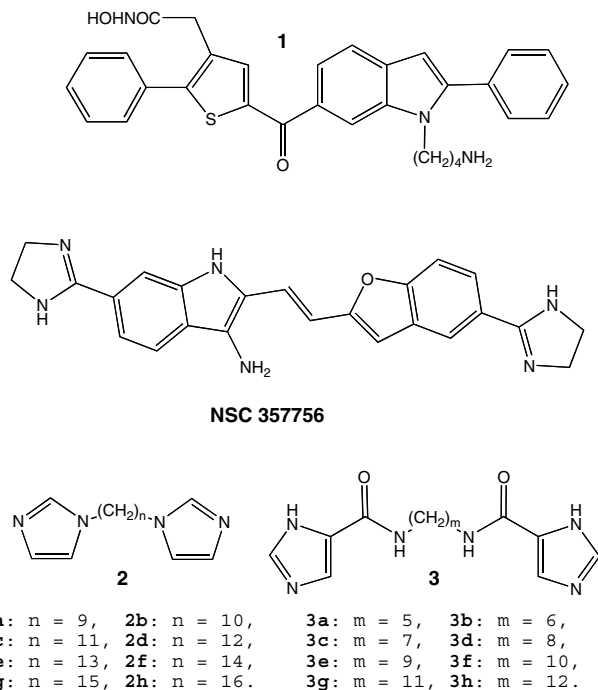


Figure 1.

**Table 1.** Inhibition of the zinc endopeptidase of botulinum neurotoxin serotype A by imidazole, its dimers (2 and 3), and NSC 357756

Inhibitor	% inhibition at 100 $\mu$ M
2a	8.2 $\pm$ 4.2 (2)
2b	19.4 $\pm$ 2.2 (2)
2c	31.0 $\pm$ 4.0 (2)
2d	56.7 $\pm$ 8.9 (2)
2e	61.0 $\pm$ 1.9 (2)
2f	56.4 $\pm$ 2.5 (2)
2g	55.9 $\pm$ 4.4 (2)
2h	58.2 $\pm$ 0.6 (2)
NSC 357756	58.4 $\pm$ 3.8 (2)
3a	1.6 $\pm$ 0.8 (3)
3b	2.3 $\pm$ 0.8 (3)
3c	4.0 $\pm$ 0.9 (3)
3d	1.9 $\pm$ 0.6 (3)
3e	2.4 $\pm$ 0.8 (3)
3f	3.6 $\pm$ 0.9 (3)
3g	5.9 $\pm$ 0.2 (3)
3h	13.0 $\pm$ 2.0 (3)
Imidazole	0

addition, the inhibition of the endopeptidase by **2a–h** depends upon linker chain length; the maximal inhibition was achieved with a chain length of 13 methylene

groups (Table 1). Compared to **2a–h**, bis-imidazoles **3a–h** exhibited much weaker inhibition of the endopeptidase at a drug concentration of 100  $\mu$ M (Table 1); maximal inhibition exhibited by the amide-containing bis-imidazole was 13% in contrast to the 61% inhibition by the amide-free bis-imidazole. Furthermore, none of bis-imidazoles **2** and **3** exhibited significant inhibition of the zinc endopeptidase from botulinum neurotoxin serotype B (data not shown), which precludes the possibility that the observed inhibition of the BoNTA activity by **2** and **3** was due to non-specific zinc chelation.

## 2.4. Modeling

Studies to predict the three-dimensional model of a bis-imidazole-bound BoNTA endopeptidase complex were performed after the experimental studies of the imidazole dimers. This was because the alkylene-linked imidazole dimers are too flexible to be docked into the active site of BoNTA using conventional docking approaches. Due to the limited computing resources, only the most potent bis-imidazole inhibitor (**2e**) developed in this study was docked to BoNTA using a three-step, divide-and-conquer docking strategy (manuscript in preparation). In the computationally predicted model, dimer **2e** spans the active site of the endopeptidase with one imidazole coordinating the zinc ion and the other imidazole simultaneously interacting favorably with the carboxylate of Glu54 (Fig. 2). The distance between the zinc ion and the nitrogen atom at position-3 of the imidazole inside the active site is 2.1 Å, while the distances of the nitrogen atom at position-3 of the other imidazole to the two carboxylate oxygen atoms of Glu54 are 2.93 and 2.67 Å. The 12 torsions of the alkylene linker as defined in Figure 2 are  $-153$ ,  $-176$ ,  $-171$ ,  $145$ ,  $97$ ,  $135$ ,  $-149$

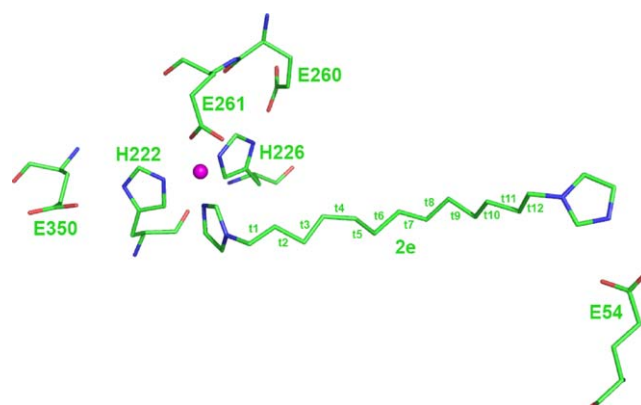


Figure 2.

170, –168, –179, 174, and –176 degrees of arc, respectively. Assuming that the methylene group attached to the zinc-bound imidazole is the first methylene group, the third and sixth methylene groups have favorable van der Waals interactions with the methylene group of Glu163.

### 3. Discussion

#### 3.1. Peripheral site for imidazolium

The endopeptidase inhibition assays showed that the maximal inhibition was achieved when the two imidazoles of **2** were tethered with 13 methylene groups, and that the inhibition was reduced when the imidazoles were linked with more or less than 13 methylene groups. The results indicate that **2e**, which contains a 13 methylene linker, inhibits the endopeptidase in a two-site binding mode. Consistent with the results of the inhibition assays, independent computational studies suggest that **2e** is able to span the active site of the endopeptidase with one imidazole coordinating the zinc ion and the other imidazole simultaneously interacting favorably with the carboxylate of Glu54 (Fig. 2). The computationally predicted ionic interaction of **2e** with Glu54 is supported by our measured  $pK_a$  value ( $6.68 \pm 0.03$ ) of **2e**. Relative to a typical  $pK_a$  value (4.4) of a glutamate,<sup>32</sup> the  $pK_a$  value of **2e** enables the imidazole in **2e** to form a salt bridge with Glu54. The involvement of Glu54 is further supported by our measured  $pK_a$  value ( $4.05 \pm 0.03$ ) of **3h**, the most potent of the **3** series. The more acidic  $pK_a$  value of **3h** impairs the ionic interaction of **3h** with Glu54 thus disabling the two-site binding of **3h**. Like imidazole alone, **3h** and its homologues are poor inhibitors of the endopeptidase due to their inability to interact with Glu54, despite the fact that the imidazole group in **3** is a better zinc coordinator than that in **2**. The latter is because only the imidazole group in **3** is in an equilibrium with imidazolium that has a higher affinity for zinc than imidazole according to the quantum chemical calculations.<sup>33</sup> In view of these results, we propose that the endopeptidase of BoNTA has a peripheral site for imidazolium binding near Glu54.

#### 3.2. Bivalence approach to BoNTA Inhibitors

It is interesting to note that NSC 357756, the second most potent small-molecule inhibitor identified from high-throughput screen of 1990 chemicals deposited at National Cancer Institute (NCI) diversity set,<sup>6</sup> showed 58% inhibition of the endopeptidase at the same assay condition used for testing bis-imidazoles **2** and **3** (Table 1). Simply coupling two imidazoles with a 13 methylene linker resulted in an endopeptidase inhibitor that is as potent as NSC 357756, an inhibitor that was identified through the labor-intensive effort of screening the NCI diversity set. This result demonstrates the power of the bivalence approach and encourages its application to the development of small-molecule endopeptidase inhibitors. Specifically, it suggests that the amino group of inhibitor **1** be replaced by an imidazole group with a chain that is long enough to permit the hydroxamate

group to coordinate the zinc ion and the imidazole group to interact with Glu54, given the advantage of the imidazole group described in Section 2.1. It also suggests that dimer **2e** can be improved by replacing the *N*-alkylimidazole with a better zinc coordinate such as 2-mercapto-3-phenylpropanamide.<sup>34</sup>

### 4. Methods and materials

#### 4.1. Synthesis

Melting points are uncorrected. Infrared spectra were recorded on a Thermo Nicolet Avatar 370 FT-IR. <sup>1</sup>H NMR spectra were recorded on a Varian Mercury 400 (400 MHz) spectrometer. <sup>13</sup>C NMR spectra were recorded on a Varian Mercury 400 (100 MHz) spectrometer. Chemical shifts are reported in ppm from the solvent resonance as the internal standard. Data are reported as follows: chemical shift, multiplicity (s, single; d, doublet; t, triplet; qr, quartet; qn, quintet, br, broad; and m, multiplet), coupling constants (Hz), and integration. Mass spectra were obtained on an HP5973 mass-selective detector with an SIS DIP-MS. Elemental analyses were performed by Atlantic Microlab, Inc. (Norcross, Georgia). Anhydrous THF and CH<sub>2</sub>Cl<sub>2</sub> were obtained through activated alumina columns by the Solv-Tech Inc. Anhydrous DMF was obtained by distillation from CaH<sub>2</sub> under N<sub>2</sub>. All other commercially obtained reagents were used as received. Flash chromatography was performed on silica gel 60 (EM Science, 230–400 mesh).

**4.1.1. General procedure for bis-(*O*-tosyl)alkanes (**5**). A solution of diol **4** (4.0 mmol), *N*-methyl morpholine (16.0 mmol), and *p*-tosyl chloride (8.8 mmol) in 25 mL of anhydrous THF was stirred at room temperature for 1–5 days. The solvent was then removed under reduced pressure, and the mixture was dissolved in dichloromethane, washed with 1 N NaHCO<sub>3</sub> (3 × 50 mL), 1 N HCl (3 × 50 mL), and deionized water (3 × 50 mL), respectively. The organic phase was dried with anhydrous Na<sub>2</sub>SO<sub>4</sub>, filtered, and concentrated under reduced pressure. The resulting mixture was purified by column chromatography (hexanes/ethyl acetate 3:1) to give **2**.**

**4.1.2. 1,9-Bis-(*O*-tosyl)nonane (**5a**).<sup>19,20,28,29</sup> Yield: 75%; white powder; mp 75–76 °C; IR (KBr) cm<sup>-1</sup> 3069, 2941, 2849, 1466, 825, 663; <sup>1</sup>H NMR (400 MHz, CDCl<sub>3</sub>) δ 1.21–1.28 (m, 10H), 1.61 (qn, *J* = 7.2 Hz, 4H), 2.45 (s, 6H), 4.00 (t, *J* = 6.4 Hz, 4H), 7.34 (d, *J* = 8.0 Hz, 4H), 7.78 (d, *J* = 8.4 Hz, 4H); <sup>13</sup>C NMR (100 MHz, CDCl<sub>3</sub>) δ 21.88, 25.50, 28.98, 29.00, 29.14, 29.33, 70.86, 128.11, 130.04, 133.41, 144.89; LREIMS C<sub>23</sub>H<sub>32</sub>O<sub>6</sub>S<sub>2</sub> requires 468.16. Found 468 ([M<sup>+</sup>], 3%), 91 ([C<sub>7</sub>H<sub>7</sub><sup>+</sup>], 100%); Anal. Calcd for C<sub>23</sub>H<sub>32</sub>O<sub>6</sub>S<sub>2</sub>: C, 58.95; H, 6.88; N, 0.00. Found: C, 59.06; H, 7.01; N 0.00.**

**4.1.3. 1,12-Bis-(*O*-tosyl)dodecane (**5d**).<sup>21–23,28,29</sup> Yield: 80%; white powder; mp 68–69 °C; IR (KBr) cm<sup>-1</sup> 2926, 2853, 1358, 843, 669; <sup>1</sup>H NMR (400 MHz, CDCl<sub>3</sub>) δ 1.21–1.27 (m, 16H), 1.63 (qn, *J* = 7.1 Hz, 4H), 2.45 (s, 6H), 4.01 (t, *J* = 6.4 Hz, 4H), 7.34 (d, *J* = 8.0 Hz, 4H),**

7.79 (d,  $J = 9.2$  Hz, 4H);  $^{13}\text{C}$  NMR (100 MHz,  $\text{CDCl}_3$ )  $\delta$  21.65, 25.33, 28.82, 28.92, 29.34, 29.41, 70.71, 127.89, 129.81, 133.22, 144.63; LREIMS  $\text{C}_{26}\text{H}_{38}\text{O}_6\text{S}_2$  requires 510.21. Found 510 ( $[\text{M}^+]$ , 4%), 91 ( $[\text{C}_7\text{H}_7^+]$ , 100%); Anal. Calcd for  $\text{C}_{26}\text{H}_{38}\text{O}_6\text{S}_2$ : C, 61.15; H, 7.50; N, 0.00. Found: C, 61.08; H, 7.47; N, 0.00.

**4.1.4. 1,15-Bis-(*O*-tosyl)pentadecane (5g).**<sup>25</sup> Yield: 67%; white powder; mp 72–73 °C; IR (KBr)  $\text{cm}^{-1}$  2977, 2923, 2850, 1354, 839, 669;  $^1\text{H}$  NMR (100 MHz,  $\text{CDCl}_3$ )  $\delta$  1.21–1.31 (m, 20H), 1.63 (qn,  $J = 7.1$  Hz, 4H), 2.45 (s, 6H), 4.01 (t,  $J = 6.6$  Hz, 4H), 7.34 (d,  $J = 8.8$  Hz, 4H), 7.79 (d,  $J = 8.4$  Hz, 4H);  $^{13}\text{C}$  NMR (100 MHz,  $\text{CDCl}_3$ )  $\delta$  21.88, 25.55, 29.04, 29.16, 29.61, 29.72, 29.81, 29.84, 70.95, 128.12, 130.03, 133.42, 144.85; LREIMS  $\text{C}_{29}\text{H}_{44}\text{O}_6\text{S}_2$  requires 552.26. Found 552 ( $[\text{M}^+]$ , 5%), 91 ( $[\text{C}_7\text{H}_7^+]$ , 100%); Anal. Calcd for  $\text{C}_{29}\text{H}_{44}\text{O}_6\text{S}_2$ : C, 63.01; H, 8.02; N, 0.00. Found: C, 63.12; H, 8.00; N, 0.00.

**4.1.5. 1,16-Bis-(*O*-tosyl)hexadecane (5h).**<sup>24,26–28</sup> Yield: 90%; white powder; mp 79–81 °C; IR (KBr)  $\text{cm}^{-1}$  2977, 2923, 2851, 1358, 838, 670;  $^1\text{H}$  NMR (100 MHz,  $\text{CDCl}_3$ )  $\delta$  1.21–1.31 (m, 22H), 1.63 (qn,  $J = 7.2$  Hz, 4H), 2.45 (s, 6H), 4.02 (t,  $J = 6.4$  Hz, 4H), 7.34 (d,  $J = 8.0$  Hz, 4H), 7.79 (d,  $J = 8.0$  Hz, 4H);  $^{13}\text{C}$  NMR (100 MHz,  $\text{CDCl}_3$ )  $\delta$  21.65, 25.34, 28.83, 28.94, 29.40, 29.50, 29.60, 29.64, 70.72, 127.90, 129.80, 133.27, 144.62; LREIMS  $\text{C}_{30}\text{H}_{46}\text{O}_6\text{S}_2$  requires 566.27. Found 566 ( $[\text{M}^+]$ , 32%), 91 ( $[\text{C}_7\text{H}_7^+]$ , 100%); Anal. Calcd for  $\text{C}_{30}\text{H}_{46}\text{O}_6\text{S}_2$ : C, 63.57; H, 8.18; N, 0.00. Found: C, 63.42; H, 8.25; N, 0.00.

**4.1.6. 1-Bromo-13-(*O*-tosyl)tridecane (7e).** A solution of 13-bromotridecanol-1 **6e** (2.5 mmol), *N*-methylmorpholine (5.0 mmol), and *p*-tosyl chloride (2.6 mmol) in 25 mL of anhydrous THF was stirred at room temperature for 2 days. The solvent was then removed under reduced pressure, and the mixture was dissolved in dichloromethane, washed with 1 N  $\text{NaHCO}_3$  (3  $\times$  50 mL), 1 N HCl (3  $\times$  50 mL), and deionized water (3  $\times$  50 mL), respectively. The organic phase was dried with anhydrous  $\text{Na}_2\text{SO}_4$ , filtered, and concentrated under reduced pressure. The resulting mixture was purified by column chromatography (hexanes/ethyl acetate 3:1) to give **7e** in 45% yield; white powder; mp 44–45 °C; IR (KBr)  $\text{cm}^{-1}$  2920, 2953, 1597, 1354, 846, 665;  $^1\text{H}$  NMR (400 MHz,  $\text{CDCl}_3$ )  $\delta$  1.21–1.27 (m, 16H), 1.42 (qn,  $J = 7.2$  Hz, 2H), 1.63 (qn,  $J = 7.0$  Hz, 2H), 1.85 (qn,  $J = 7.2$  Hz, 2H), 2.45 (s, 3H), 3.41 (t,  $J = 6.8$  Hz, 2H), 4.02 (t,  $J = 6.4$  Hz, 2H), 7.34 (d,  $J = 8.2$  Hz, 2H), 7.79 (d,  $J = 8.6$  Hz, 2H);  $^{13}\text{C}$  NMR (100 MHz,  $\text{CDCl}_3$ )  $\delta$  21.65, 25.32, 28.16, 28.76, 28.81, 28.91, 29.37, 29.42, 29.45, 29.50, 29.53, 32.83, 34.10, 70.71, 127.89, 129.79, 133.22, 144.62; LREIMS  $\text{C}_{20}\text{H}_{33}\text{BrO}_3\text{S}$  requires 434.13. Found 435 ( $[\text{M}^+]$ , 30%), 433 ( $[\text{M}^+]$ , 30%), 263 ( $[\text{M}-\text{TsO}^+]$ , 99%), 261 ( $[\text{M}-\text{TsO}^+]$ , 100%); Anal. Calcd for  $\text{C}_{20}\text{H}_{33}\text{BrO}_3\text{S}$ : C, 55.42; H, 7.67; N, 0.00; Found: C, 55.58; H, 7.71; N 0.00.

**4.1.7. General procedure for bis-(*N*-imidazolyl)alkanes 2.** A mixture of bis-tosylalkane **5**, dibromoalkane **8**, or tosylbromoalkane **7** (2.0 mmol) and imidazole sodium salt (4.4 mmol) in 15 mL of anhydrous DMF was stirred

at room temperature overnight. The solvent was removed by distillation at reduced pressure. The resulting brown syrup was purified by column chromatography with silica gel 50% of which was saturated with  $\text{NH}_3$  gas (Typical solvent system: dichloromethane/MeOH (97/3)).

**4.1.8. General procedure for bis-(*N*-imidazolyl)alkane hydrochloride salts 2.** A solution of bis-(*N*-imidazolyl)alkane **2** (0.5 mmol) in 5 mL of anhydrous THF was purged with HCl gas for 10–15 s. The solvent was removed under reduced pressure and the hydrochloride salt of **2** was dried under high vacuum at 70 °C.

**4.1.9. 1,9-Bis-(imidazol-1-yl)nonane dihydrochloride (2a).** Yield: 37%; colorless oil; IR (KBr)  $\text{cm}^{-1}$  3100, 2930, 2856, 1575, 1457, 629;  $^1\text{H}$  NMR (400 MHz,  $\text{DMSO}-d_6$ )  $\delta$  1.20–1.37 (m, 10H), 1.78 (qn,  $J = 6.8$  Hz, 4H), 4.16 (t,  $J = 7.0$  Hz, 4H), 7.68 (s, 2H), 7.79 (s, 2H), 9.21 (s, 2H);  $^{13}\text{C}$  NMR (100 MHz,  $\text{DMSO}-d_6$ )  $\delta$  26.21, 29.03, 29.43, 30.16, 49.13, 120.12, 122.66, 135.83; LREIMS  $\text{C}_{15}\text{H}_{24}\text{N}_4$  (neutral form) requires 260.20. Found 259 ( $[\text{M}-\text{H}^+]$ , 35%), 179 ( $[\text{M}-(\text{N-methyleneimidazole})^+]$ , 100%); Anal. Calcd for  $\text{C}_{15}\text{H}_{26}\text{Cl}_2\text{N}_4 \cdot 2\text{H}_2\text{O}$ : C, 48.78; H, 8.19; N, 15.17. Found: C, 48.99; H, 8.12; N, 14.87.

**4.1.10. 1,10-Bis-(imidazol-1-yl)decane dihydrochloride (2b).** Yield: 45%; white powder; mp 132–134 °C; IR (KBr)  $\text{cm}^{-1}$  3068, 3022, 2932, 2857, 1545, 865, 636;  $^1\text{H}$  NMR (400 MHz,  $\text{DMSO}-d_6$ )  $\delta$  1.15–1.25 (m, 12H), 1.77 (qn,  $J = 6.8$  Hz, 4H), 4.16 (t,  $J = 7.0$  Hz, 4H), 7.68 (d,  $J = 1.2$  Hz, 2H), 7.79 (d,  $J = 1.2$  Hz, 2H), 9.18 (s, 2H);  $^{13}\text{C}$  NMR (100 MHz,  $\text{DMSO}-d_6$ )  $\delta$  26.24, 29.03, 29.47, 30.15, 49.10, 120.14, 122.63, 135.87; LREIMS  $\text{C}_{16}\text{H}_{26}\text{N}_4$  (neutral form) requires 274.22. Found 273 ( $[\text{M}-\text{H}^+]$ , 51%), 193 ( $[\text{M}-(\text{N-methyleneimidazole})^+]$ , 100%); Anal. Calcd for  $\text{C}_{16}\text{H}_{28}\text{Cl}_2\text{N}_4$ : C, 55.33; H, 8.13; N, 16.13. Found: C, 55.09; H, 8.12; N, 15.74.

**4.1.11. 1,11-Bis-(imidazol-1-yl)undecane dihydrochloride (2c).** Yield: 43%; white powder; mp 138–139 °C; IR (KBr)  $\text{cm}^{-1}$  3392, 2928, 2856, 1576, 1547, 764, 628;  $^1\text{H}$  NMR (400 MHz,  $\text{DMSO}-d_6$ )  $\delta$  1.15–1.25 (m, 14H), 1.77 (qn,  $J = 7.0$  Hz, 4H), 4.17 (t,  $J = 7.0$  Hz, 4H), 7.68 (d,  $J = 1.6$  Hz, 2H), 7.79 (d,  $J = 1.6$  Hz, 2H), 9.21 (s, 2H);  $^{13}\text{C}$  NMR (100 Hz,  $\text{DMSO}-d_6$ )  $\delta$  26.23, 29.06, 29.57, 30.12, 49.14, 120.43, 122.65, 135.85; LREIMS  $\text{C}_{17}\text{H}_{28}\text{N}_4$  (neutral form) requires 288.23. Found 287 ( $[\text{M}-\text{H}^+]$ , 51%), 207 ( $[\text{M}-(\text{N-methyleneimidazole})^+]$ , 100%); Anal. Calcd for  $\text{C}_{17}\text{H}_{30}\text{Cl}_2\text{N}_4 \cdot \text{H}_2\text{O}$ : C, 53.82; H, 8.50; N, 14.77. Found: C, 53.68; H, 8.49; N, 14.38.

**4.1.12. 1,12-Bis-(imidazol-1-yl)dodecane dihydrochloride (2d).** Yield: 32%; white powder; mp 127–129 °C; IR (KBr)  $\text{cm}^{-1}$  2923, 2854, 1472, 662;  $^1\text{H}$  NMR (400 MHz,  $\text{DMSO}-d_6$ )  $\delta$  1.15–1.25 (m, 16H), 1.72 (qn,  $J = 7.2$  Hz, 4H), 4.05 (t,  $J = 7.2$  Hz, 4H), 7.31 (d,  $J = 1.6$  Hz, 2H), 7.50 (d,  $J = 1.6$  Hz, 2H), 8.48 (s, 2H);  $^{13}\text{C}$  NMR (100 MHz,  $\text{DMSO}-d_6$ )  $\delta$  26.47, 29.13, 29.58, 29.67, 30.64, 48.29, 121.41, 124.22, 136.74; LREIMS  $\text{C}_{18}\text{H}_{30}\text{N}_4$  (neutral form) requires 302.25. Found 301 ( $[\text{M}-\text{H}^+]$ , 92%), 221 ( $[\text{M}-(\text{N-methyleneimidazole})^+]$ ,

100%); Anal. Calcd for  $C_{18}H_{32}Cl_2N_4 \cdot 0.5H_2O$ : C, 56.24; H, 8.65; N, 14.58. Found: C, 56.43; H, 8.64; N, 14.26.

**4.1.13. 1,13-Bis-(imidazol-1-yl)tridecane dihydrochloride (2e).** Yield: 39%; white powder; mp 117–118 °C; IR (KBr)  $cm^{-1}$  2921, 2853, 1567, 1474, 796, 636;  $^1H$  NMR (400 MHz, DMSO- $d_6$ )  $\delta$  1.15–1.25 (m, 16H), 1.72 (qn,  $J = 7.2$  Hz, 4H), 4.05 (t,  $J = 7.2$  Hz, 4H), 7.31 (d,  $J = 1.6$  Hz, 2H), 7.50 (d,  $J = 1.6$  Hz, 2H), 8.48 (s, 2H);  $^{13}C$  NMR (100 MHz, DMSO- $d_6$ )  $\delta$  26.43, 29.12, 29.54, 29.61, 30.68, 48.24, 121.42, 124.25, 136.75; LREIMS  $C_{19}H_{32}N_4$  (neutral form) requires 316.26. Found 315 ( $[M-H]^+$ , 69%), 235 ( $[M-(N\text{-methyleneimidazole})^+]$ , 100%); Anal. Calcd for  $C_{19}H_{34}Cl_2N_4 \cdot 0.4H_2O$ : C, 56.24; H, 8.65; N, 14.58. Found: C, 56.43; H, 8.64; N, 14.26.

**4.1.14. 1,14-Bis-(imidazol-1-yl)tetradecane dihydrochloride (2f).** Yield: 41%; white powder; mp 150–152 °C; IR (KBr)  $cm^{-1}$  3091, 3021, 2925, 2852, 1575, 1463, 868, 641;  $^1H$  NMR (400 MHz, DMSO- $d_6$ )  $\delta$  1.11–1.31 (m, 18H), 1.78 (qn,  $J = 7.2$  Hz, 4H), 4.17 (t,  $J = 7.0$  Hz, 4H), 7.68 (s, 2H), 7.80 (s, 2H), 9.24 (s, 2H);  $^{13}C$  NMR (100 MHz, DMSO- $d_6$ )  $\delta$  26.74, 29.23, 29.62, 29.78, 31.46, 47.75, 119.36, 128.04, 136.92; LREIMS  $C_{20}H_{34}N_4$  (neutral form) requires 330.28. Found 329 ( $[M-H]^+$ , 76%), 249 ( $[M-(N\text{-methyleneimidazole})^+]$ , 100%); Anal. Calcd for  $C_{20}H_{36}Cl_2N_4 \cdot 0.75H_2O$ : C, 57.61; H, 9.07; N, 13.44. Found: C, 57.86; H, 9.00; N, 13.22.

**4.1.15. 1,15-Bis-(imidazol-1-yl)pentadecane dihydrochloride (2g).** Yield: 45%; white powder; mp 143–145 °C; IR (KBr)  $cm^{-1}$  3091, 2928, 2851, 1574, 1462, 640;  $^1H$  NMR (400 MHz, DMSO- $d_6$ )  $\delta$  1.11–1.31 (m, 20H), 1.78 (qn,  $J = 7.2$  Hz, 4H), 4.16 (t,  $J = 7.2$  Hz, 4H), 7.68 (s, 2H), 7.78 (s, 2H), 9.18 (s, 2H);  $^{13}C$  NMR (100 MHz, DMSO- $d_6$ )  $\delta$  26.49, 29.32, 29.80, 29.91, 29.99, 30.01, 30.36, 49.40, 120.74, 122.90, 136.04; LREIMS  $C_{21}H_{36}N_4$  (neutral form) requires 344.29. Found 343 ( $[M-H]^+$ , 75%), 263 ( $[M-(N\text{-methyleneimidazole})^+]$ , 100%); Anal. Calcd for  $C_{21}H_{39}Cl_2N_4 \cdot 0.25H_2O$ : C, 59.77; H, 9.20; N, 13.28. Found: C, 59.77; H, 9.20; N, 13.00.

**4.1.16. 1,16-Bis-(imidazol-1-yl)hexadecane dihydrochloride (2h).** Yield: 90%; white powder; mp 137–138 °C; IR (KBr)  $cm^{-1}$  2920, 2850, 1585, 1471, 654;  $^1H$  NMR (400 MHz, DMSO- $d_6$ )  $\delta$  1.11–1.31 (m, 22H), 1.78 (qn,  $J = 7.2$  Hz, 4H), 4.16 (t,  $J = 7.2$  Hz, 4H), 7.68 (s, 2H), 7.78 (s, 2H), 9.18 (s, 2H);  $^{13}C$  NMR (100 MHz, DMSO- $d_6$ )  $\delta$  26.23, 29.05, 29.54, 29.65, 29.72, 29.76, 30.10, 49.15, 120.50, 122.63, 135.78; LREIMS  $C_{22}H_{38}N_4$  (neutral form) requires 358.31. Found 357 ( $[M-H]^+$ , 68%), 277 ( $[M-(N\text{-methyleneimidazole})^+]$ , 100%); Anal. Calcd for  $C_{22}H_{40}Cl_2N_4$ : C, 61.24; H, 9.34; N, 12.98. Found: C, 61.01; H, 9.45; N, 12.81.

**4.1.17. *N*-Succinimidyl-4-(5)-imidazolecarboxylate (10).** A solution of imidazole-4-(5)-carboxylate **9** (50 mmol), EDCI (50 mmol), *N*-methylmorpholine (100 mmol), and *N*-hydroxysuccinimide (50 mmol) in 60 mL of anhydrous *N,N*-DMF was stirred at room temperature for 2 days. The solvent was then removed under reduced pressure. The resulting mixture was dissolved in dichloro-

methane (100 mL), washed with 1 N  $NaHCO_3$  (3 $\times$  50 mL), 1 N HCl (3 $\times$  50 mL), and deionized water (3 $\times$  50 mL), respectively. The organic phase was dried with anhydrous  $Na_2SO_4$ , filtered, and concentrated under reduced pressure. The resulting mixture was purified by column chromatography (hexanes/ethyl acetate 3:1) to give **10** in 83% yield; white powder; mp 188–190 °C; IR (KBr)  $cm^{-1}$  3162, 3012, 2962, 2820, 2661, 1735, 1197, 943, 659;  $^1H$  NMR (400 MHz, DMSO- $d_6$ ):  $\delta$  2.86 (s, 4H), 7.97 (s, 1H), 8.26 (s, 1H), 13.08 (br, 1H);  $^{13}C$  NMR (100 MHz, DMSO- $d_6$ ):  $\delta$  26.16, 127.76, 139.23, 171.29, 173.48; LREIMS  $C_8H_7N_3O_4$  requires 209.04. Found 209 ( $[M^+]$ , 14%), 95 ( $[imidazolylcarbonyl]^+$ , 100%).

**4.1.18. General procedure for bis- $\{N$ -[1*H*-imidazole-4-(5)-carboxamidol]alkanes **3**.** A solution of *N*-succinimidyl-4-(5)-imidazolecarboxylate **10** (22 mmol) and bis(amino)alkyne (10 mmol) in 20 mL of anhydrous THF was stirred at room temperature overnight. The solvent was removed by distillation at reduced pressure and the brown syrup obtained was purified by column chromatography with silica gel (Gradient dichloromethane 100%–dichloromethane/MeOH 9:1) to give **3**.

**4.1.19. General procedure for bis- $\{N$ -[1*H*-imidazole-4-(5)-carboxamidol]alkane hydrochloride salts **3**.** A solution of bis- $\{N$ -[1*H*-imidazole-4-(5)-carboxamido]alkane **3** (5 mmol) in 5 mL of anhydrous THF was purged with HCl gas for 10–15 s. The solvent was removed under reduced pressure and the hydrochloride salt of **3** was dried under high vacuum at 70 °C.

**4.1.20. 1,5-Bis- $\{N$ -[1*H*-imidazole-4-(5)-carboxamidol]-pentane hydrochloride (3a).** Yield: 58%; white powder; mp 194–195 °C; IR (KBr)  $cm^{-1}$  3245, 3091, 2868, 1651, 1543, 1326, 820, 626;  $^1H$  NMR (400 MHz, DMSO- $d_6$ )  $\delta$  1.39 (qn,  $J = 7.2$  Hz, 2H), 1.56 (qn,  $J = 7.2$  Hz, 4H), 3.26 (qr,  $J = 6.4$  Hz, 4H), 8.88 (s, 2H), 9.09–9.13 (m, 2H);  $^{13}C$  NMR (100 MHz, DMSO- $d_6$ )  $\delta$  23.79, 28.45, 38.49, 120.17, 128.03, 135.59, 156.96; LREIMS  $C_{13}H_{18}N_6O_2$  (neutral form) requires 290.15. Found 290 ( $[M^+]$ , 9%), 95 ( $[imidazolylcarbonyl]^+$ , 100%); Anal. Calcd for  $C_{13}H_{20}Cl_2N_6O_2 \cdot 0.25H_2O$ : C, 42.46; H, 5.61; N, 22.86. Found: C, 42.73; H, 5.62; N, 22.57.

**4.1.21. 1,6-Bis- $\{N$ -[1*H*-imidazole-4-(5)-carboxamidol]-hexane hydrochloride (3b)**<sup>35</sup>. Yield: 24%; white powder; mp 258–260 °C; IR (KBr)  $cm^{-1}$  3234, 3062, 2935, 2869, 1667, 1552, 1448, 827, 629;  $^1H$  NMR (400 MHz, DMSO- $d_6$ )  $\delta$  1.30–1.35 (m, 4H), 1.52 (qn,  $J = 6.0$  Hz, 4H), 3.25 (qr,  $J = 6.4$  Hz, 4H), 8.30 (s, 2H), 9.08 (br, 2H), 9.10 (s, 2H);  $^{13}C$  NMR (100 MHz, DMSO- $d_6$ )  $\delta$  26.05, 28.83, 38.68, 120.10, 128.28, 135.60, 157.10; LREIMS  $C_{14}H_{20}N_6O_2$  (neutral form) requires 304.16. Found 304 ( $[M^+]$ , 6%), 95 ( $[imidazolylcarbonyl]^+$ , 100%); Anal. Calcd for  $C_{14}H_{22}Cl_2N_6O_2 \cdot 0.75H_2O$ : C, 43.03; H, 6.06; N, 21.51. Found: C, 43.16; H, 6.19; N, 21.17.

**4.1.22. 1,7-Bis- $\{N$ -[1*H*-imidazole-4-(5)-carboxamidol]-heptane hydrochloride (3c).** Yield: 33%; white powder; mp 176–178 °C; IR (KBr)  $cm^{-1}$  3254, 3096, 3019, 2854, 1684, 1559, 1341, 842, 629;  $^1H$  NMR (400 MHz,

DMSO- $d_6$ )  $\delta$  1.25–1.34 (m, 6H), 1.51 (qn,  $J$  = 6.0 Hz, 4H), 3.25 (qr,  $J$  = 6.6 Hz, 4H), 8.21 (s, 2H), 8.93 (t,  $J$  = 5.4 Hz, 2H), 9.04 (s, 2H);  $^{13}\text{C}$  NMR (100 MHz, DMSO- $d_6$ ):  $\delta$  26.37, 28.41, 28.89, 38.75, 120.02, 128.45, 135.68, 157.23; LREIMS  $\text{C}_{15}\text{H}_{22}\text{N}_6\text{O}_2$  (neutral form) requires 318.18. Found 318 ( $[\text{M}^+]$ , 10%), 95 ([imidazolylcarbonyl] $^+$ , 100%); Anal. Calcd for  $\text{C}_{15}\text{H}_{24}\text{Cl}_2\text{N}_6\text{O}_2 \cdot 0.75\text{H}_2\text{O}$ : C, 44.51; H, 6.34; N, 20.76. Found: C, 44.58; H, 6.53; N, 20.46.

**4.1.23. 1,8-Bis- $\{N$ -[1*H*-imidazole-4-(5)-carboxamidol]-octane hydrochloride (3d).** Yield: 41%; white powder; mp 143–144 °C; IR (KBr)  $\text{cm}^{-1}$  3254, 3101, 2929, 2853, 1683, 1560, 1339, 831, 629;  $^1\text{H}$  NMR (400 MHz, DMSO- $d_6$ )  $\delta$  1.19–1.30 (m, 8H), 1.46 (qn,  $J$  = 6.0 Hz, 4H), 3.16 (qr,  $J$  = 6.7 Hz, 4H), 7.55 (s, 2H), 7.67 (s, 2H), 7.83 (s, 2H), 12.40 (br, 2H);  $^{13}\text{C}$  NMR (100 MHz, DMSO- $d_6$ )  $\delta$  26.34, 28.63, 28.85, 38.74, 120.09, 128.26, 135.56, 157; LREIMS  $\text{C}_{16}\text{H}_{24}\text{N}_6\text{O}_2$  (neutral form) requires 332.20. Found 332 ( $[\text{M}^+]$ , 10%), 95 ([imidazolylcarbonyl] $^+$ , 100%); Anal. Calcd for  $\text{C}_{16}\text{H}_{26}\text{Cl}_2\text{N}_6\text{O}_2$ : C, 47.41; H, 6.47; N, 20.73. Found: C, 47.03; H, 6.81; N, 20.43.

**4.1.24. 1,9-Bis- $\{N$ -[1*H*-imidazole-4-(5)-carboxamidol]-nonane hydrochloride (3e).** Yield: 23%; white powder; mp 152–154 °C; IR (KBr)  $\text{cm}^{-1}$  3246, 3088, 2928, 2849, 1669, 1560, 1336, 846, 629;  $^1\text{H}$  NMR (400 MHz, DMSO- $d_6$ )  $\delta$  1.21–1.35 (m, 10H), 1.51 (qn,  $J$  = 6.4 Hz, 4H), 3.24 (qr,  $J$  = 6.5 Hz, 4H), 8.27 (s, 2H), 9.02 (t,  $J$  = 5.4 Hz, 2H), 9.12 (s, 2H);  $^{13}\text{C}$  NMR (100 MHz, DMSO- $d_6$ )  $\delta$  26.41, 28.69, 28.87, 28.92, 38.81, 120.07, 128.07, 135.63, 156.95; LREIMS  $\text{C}_{17}\text{H}_{26}\text{N}_6\text{O}_2$  (neutral form) requires 346.21. Found 346 ( $[\text{M}^+]$ , 12%), 95 ([imidazolylcarbonyl] $^+$ , 100%); Anal. Calcd for  $\text{C}_{17}\text{H}_{28}\text{Cl}_2\text{N}_6\text{O}_2 \cdot 2\text{H}_2\text{O}$ : C, 44.84; H, 7.08; N, 18.46. Found: C, 45.12; H, 6.94; N, 18.13.

**4.1.25. 1,10-Bis- $\{N$ -[1*H*-imidazole-4-(5)-carboxamidol]-decane hydrochloride (3f).** Yield: 48%; white powder; mp 192–193 °C; IR (KBr)  $\text{cm}^{-1}$  3257, 3097, 2923, 2850, 1668, 1555, 1345, 840, 628;  $^1\text{H}$  NMR (400 MHz, DMSO- $d_6$ )  $\delta$  1.23–1.32 (m, 12H), 1.50 (qn,  $J$  = 6.0 Hz, 4H), 3.24 (qr,  $J$  = 6.4 Hz, 4H), 8.16 (s, 2H), 8.84 (s, 2H), 8.96 (s, 2H);  $^{13}\text{C}$  NMR (100 MHz, DMSO- $d_6$ )  $\delta$  25.70, 26.40, 28.72, 28.95, 38.71, 119.98, 135.66, 157.51; LREIMS  $\text{C}_{18}\text{H}_{28}\text{N}_6\text{O}_2$  (neutral form) requires 360.23. Found 360 ( $[\text{M}^+]$ , 12%), 95 ([imidazolylcarbonyl] $^+$ , 100%); Anal. Calcd for  $\text{C}_{18}\text{H}_{30}\text{Cl}_2\text{N}_6\text{O}_2 \cdot 0.75\text{H}_2\text{O}$ : C, 48.38; H, 7.10; N, 18.81. Found: C, 48.59; H, 7.28; N, 18.51.

**4.1.26. 1,11-Bis- $\{N$ -[1*H*-imidazole-4-(5)-carboxamidol]-undecane hydrochloride (3g).** Yield: 53%; white powder; mp 194–196 °C; IR (KBr)  $\text{cm}^{-1}$  3337, 3096, 2922, 2849, 1649, 1556, 1343, 839, 628;  $^1\text{H}$  NMR (400 MHz, DMSO- $d_6$ )  $\delta$  1.21–1.35 (m, 14H), 1.49 (qn,  $J$  = 6.0 Hz, 4H), 3.23 (qr,  $J$  = 6.3 Hz, 4H), 8.07 (s, 2H), 8.70–8.72 (m, 4H);  $^{13}\text{C}$  NMR (100 MHz, DMSO- $d_6$ )  $\delta$  26.43, 28.76, 29.00, 29.04, 38.62, 120.04, 130.15, 135.65, 158.36; LREIMS  $\text{C}_{19}\text{H}_{30}\text{N}_6\text{O}_2$  (neutral form) requires 374.24. Found 374 ( $[\text{M}^+]$ , 15%), 95 ([imidazolylcarbonyl] $^+$ , 100%); Anal. Calcd for  $\text{C}_{19}\text{H}_{32}\text{Cl}_2\text{N}_6\text{O}_2$ : C, 51.01; H, 7.21; N, 18.78. Found: C, 50.91; H, 7.59; N, 18.64.

**4.1.27. 1,12-Bis- $\{N$ -[1*H*-imidazole-4-(5)-carboxamidol]-dodecane hydrochloride (3h).** Yield: 23%; white powder; mp 201–203 °C; IR (KBr)  $\text{cm}^{-1}$  3298, 3087, 2919, 2851, 1659, 1576, 841, 625;  $^1\text{H}$  NMR (400 MHz, DMSO- $d_6$ )  $\delta$  1.21–1.32 (m, 16H), 1.50 (qn,  $J$  = 6.4 Hz, 4H), 3.24 (qr,  $J$  = 6.4 Hz, 4H), 8.22 (s, 2H), 8.94 (t,  $J$  = 5.4 Hz, 2H), 9.06 (s, 2H);  $^{13}\text{C}$  NMR (100 MHz, DMSO- $d_6$ )  $\delta$  26.42, 28.74, 28.90, 29.01, 29.02, 38.78, 120.03, 128.41, 135.64, 157.18; LREIMS  $\text{C}_{20}\text{H}_{32}\text{N}_6\text{O}_2$  (neutral form) requires 388.26. Found 388 ( $[\text{M}^+]$ , 10%), 95 ([imidazolylcarbonyl] $^+$ , 100%); Anal. Calcd for  $\text{C}_{20}\text{H}_{34}\text{Cl}_2\text{N}_6\text{O}_2 \cdot 1.25\text{H}_2\text{O}$ : C, 49.64; H, 7.60; N, 17.37. Found: C, 49.65; H, 7.63; N, 17.11.

## 4.2. Botulinum neurotoxin inhibition assays

Assays of BoNTA protease activities were done at 37 °C and contained 0.5 mM substrate, 1 mM dithiothreitol, 25  $\mu\text{M}$   $\text{ZnCl}_2$ , 0.5 mg/mL bovine serum albumin, 0.5–1.5  $\mu\text{g}/\text{mL}$  recombinant BoNTA light chain, 40 mM HEPES, and 0.05% Tween, pH 7.3. Substrate for BoNTA was a peptide containing residues 187–203 of SNAP-25.<sup>30</sup> Inhibitors were dissolved in dimethylsulfoxide at 10 times the final assay concentration, then diluted into the assay mixture containing substrate, followed by addition of light chain (i.e., inhibitor and light chain were not preincubated). Assay times and light chain concentrations were adjusted so that less than 10% of the substrate was hydrolyzed. Assays were stopped by acidification with trifluoroacetic acid and analyzed by reverse-phase HPLC as described.<sup>30</sup> Elemental analyses showed that some test compounds contained small amounts of water. Such water was ignored in preparing the solutions of the test compounds as the percentages of the water content in the active inhibitors were within the system errors of the assays.

## 4.3. Modeling of the 2e-bound endopeptidase of BoNTA

**4.3.1. Modeling of bis-imidazole 2e and the zinc-bound endopeptidase.** The geometry of bis-imidazole 2e was obtained by geometry optimization at the Hartree–Fock<sup>36</sup> (HF) electronic structure level with the 6-31G(d) basis set by the Gaussian 98 Program.<sup>37,38</sup> The RESP charges and force field parameters of 2e were generated by the ANTECHAMBER module of AMBER 7 program<sup>39</sup> using the geometry optimized at the HF/6-31G(d) level. The 3D structure of a truncated, zinc-containing endopeptidase (residues 1–429, 453–471, and 497–544) was modified from an available crystal structure BoNTA (PDB code: 3BTA)<sup>40</sup> using a published procedure.<sup>7</sup>

**4.3.2. Modeling of the zinc- and 2e-bound endopeptidase.** *Step 1:* compound 2e was first divided into 1-methylimidazole and 1-dodecylimidazole. The RESP charge<sup>41</sup> on the nitrogen atom at position-3 of 1-methylimidazole was changed from  $-0.537$  to  $-1.000$ , and the RESP charges on the two neighboring carbon atoms were increased by  $+0.2315$  (the difference between 1.000 and 0.537 divided by 2) to maintain charge neutrality. 1-Methylimidazole was manually placed at the active site in such a way that the nitrogen atom at position-3 of the imidazole coordinates the zinc ion and the orien-

tation of 1-methylimidazole was made to be consistent with the geometry of histidinyll imidazoles found in a survey of crystal structures of zinc proteins with a zinc complex comprising three His residues and one Glu or Asp.<sup>18</sup> The complex generated by manual docking was optimized by performing a 50-step energy minimization on 1-methylimidazole followed by a 50-step energy minimization on the complex. The resulting complex was further optimized by a 500-ps molecular dynamics simulation.

**Step 2:** 1-dodecylimidazole was manually docked into the 1-methylimidazole-bound active site of the complex obtained at Step 1. The two fragments of dimer **2e** were converted back to dimer **2e** by removing one hydrogen atom at each end of the two 1-alkylimidazoles and constructing a covalent bond between the two terminal methylene groups. The linker conformation of dimer **2e** was fully extended at this stage. The resulting complex was optimized by the same procedures used in Step 1, except that the simulation was carried out for 1500 ps. The charge of the zinc-bound nitrogen atom remained to be  $-1.000$  at this step in order to facilitate the search of the desired linker conformation.

**Step 3:** the refined complex derived in Step 2 was refined first with a 1500-step energy minimization of the inhibitor only and then with 97 different molecular dynamics simulations (2.0 ns for each simulation with a time-step of 1.0 fs and different initial velocities). In energy minimization and molecular dynamics simulations, the RESP charges on the zinc-bound nitrogen atom and the two neighboring carbon atoms were restored. Of the 97 simulations, 27 simulations had the 1-alkyl imidazole of **2e** coordinate the zinc divalent cation ion in a four-ligand coordination state during the entire 2.0-ns simulation period, 46 simulations had the 1-alkyl imidazole replaced by Glu223, and 24 simulations had the 1-alkyl imidazole replaced by a water molecule. An average structure of 13,500 instantaneous trajectories obtained at 1.0 ps intervals during the last 500-ps period of the 27 simulations was used as a plausible 3D model of the endopeptidase in complex with **2e**.

#### 4.4. Single or multiple molecular dynamics simulations

The single or multiple molecular dynamics simulations were performed according to a published protocol<sup>7</sup> using the parallel PMEMD module of the AMBER8 program<sup>39</sup> with the Cornell et al. force field (parm99.dat).<sup>36</sup> The zinc- and **2e**-bound endopeptidase complex was neutralized with two chlorides.

#### 4.5. Determination of $pK_a$ values of **2e** and **3h**

The  $pK_a$  values were determined by pION INC (5 Constitution Way, Woburn, MA, USA 01801) using potentiometry with 30–50% MeOH as a cosolvent in three titrations. The detectable  $pK_a$  range was conservatively estimated from 4 to 10. The reported errors were three times the standard deviation that arose out of non-linear regression analysis. Two  $pK_a$  values ( $6.68 \pm 0.03$  and  $7.36 \pm 0.03$ ) were detected for **2e**. The second, relatively

basic  $pK_a$  value of **2e** resulted from the intramolecular hydrogen bond of the two terminal imidazoles. One  $pK_a$  value ( $4.05 \pm 0.03$ ) was detected for **3h**.

#### Acknowledgments

This work was supported by the Defense Advanced Research Projects Agency (DAAD19-01-1-0322), the U.S. Army Medical Research Acquisition Activity (W81XWH-04-2-0001), the National Institutes of Health/National Institute of Allergy and Infectious Diseases (2R01AI054574-02), the Aeronautical Systems Center of the High Performance Computing Modernization Program of the U.S. Department of Defense, and the University of Minnesota Supercomputing Institute. The opinions or assertions contained herein belong to the author and are not necessarily the official views of the U.S. Army, the U.S. Department of Defense, or the National Institutes of Health. We thank an anonymous reviewer of an earlier version of the manuscript for helpful comments.

#### References and notes

- Shapiro, R. L.; Hatheway, C.; Swerdlow, D. L. *Ann. Intern. Med.* **1998**, *129*, 221.
- Kessler, K. R.; Benecke, R. *Neurotoxicology* **1997**, *18*, 761.
- Springen, K.; Raymond, J.; Skipp, C.; Scelfo, J. S. *Newsweek* **2002**, 50.
- Singh, B. R. *Nat. Struct. Biol.* **2000**, *7*, 617.
- Simpson, L. L. *Pharmacol. Rev.* **1981**, *33*, 155.
- Burnett, J. C.; Schmidt, J. J.; Stafford, R. G.; Panchal, R. G.; Nguyen, T. L. *Biochem. Biophys. Res. Commun.* **2003**, *310*, 84.
- Park, J. G.; Sill, P. C.; Makiyi, E. F.; Garcia-Sosa, A. T.; Millard, C. B. *Bioorg. Med. Chem.* **2006**, *14*, 395.
- Breidenbach, M. A.; Brunger, A. T. *Nature* **2004**, *432*, 925.
- Jencks, W. P. *Proc. Natl. Acad. Sci. U.S.A.* **1981**, *78*, 4046.
- Portoghese, P. S. *J. Med. Chem.* **1992**, *35*, 1927.
- Pang, Y.-P.; Quiram, P.; Jelacic, T.; Hong, F.; Brimijoin, S. *J. Biol. Chem.* **1996**, *271*, 23646.
- Shuker, S. B.; Hajduk, P. J.; Meadows, R. P.; Fesik, S. W. *Science* **1996**, *274*, 1531.
- Carlier, P. R.; Du, D.-M.; Han, Y.-F.; Liu, J.; Perola, E. *Angew. Chem., Int. Ed.* **2000**, *39*, 1775.
- Pang, Y.-P.; Kollmeyer, T. M.; Hong, F.; Lee, J.-C.; Hammond, P. I. *Chem. Biol.* **2003**, *10*, 491.
- Pang, Y.-P. *Bioorg. Med. Chem.* **2004**, *12*, 3063.
- Ramstrom, H.; Bourotte, M.; Philippe, C.; Schmitt, M.; Haiech, J. *J. Med. Chem.* **2004**, *47*, 2264.
- Shen, X.-J.; Chen, H.-L.; Yu, F.; Zhang, Y.-C.; Yang, X.-H. *Tetrahedron Lett.* **2004**, *45*, 6813.
- Roe, R. R.; Pang, Y.-P. *J. Mol. Model.* **1999**, *5*, 134.
- Laakso, T. M.; Reynolds, D. D. *J. Am. Chem. Soc.* **1951**, *73*, 3518.
- Butler, G. B.; Angelo, R. J. *J. Am. Chem. Soc.* **1956**, *78*, 4797.
- Fear, E. J. P.; Thrower, J.; Veitch, J. *J. Chem. Soc.* **1958**, 1322.
- Wittig, G.; Grolig, J. E. *Chem. Ber.* **1961**, *94*, 2148.
- Gerdil, R. *Helv. Chem. Acta* **1973**, *56*, 1859.
- Kuck, D.; Gruetzmacher, H. F. *Z. Naturforsch., B: Chem. Sci.* **1979**, *34B*, 1750.

25. Prakash, C.; Saleh, S.; Taber, D. F.; Blair, I. A. *Lipids* **1989**, *24*, 786.
26. Schlosser, M.; Bossert, H. *Tetrahedron* **1991**, *47*, 6287.
27. Munoz, S.; Mallen, J. V.; Nakano, A.; Chen, Z.; Gay, I. *J. Chem. Soc., Chem. Commun.* **1992**, 520.
28. Hogan, J. C.; Gandour, R. D. *J. Org. Chem.* **1992**, *57*, 55.
29. Pang, Y. P.; Hong, F.; Quiram, P.; Jelacic, T. *J. Chem. Soc., Perkin Trans. 1* **1997**, 171.
30. Schmidt, J. J.; Bostian, K. A. *J. Protein Chem.* **1997**, *16*, 19.
31. Schmidt, J. J.; Stafford, R. G. *Appl. Environ. Microbiol.* **2003**, *69*, 297.
32. Stryer, L. *Biochemistry*, 4th ed.; W.H. Freeman and Company: New York, 1995.
33. El Yazal, J.; Pang, Y.-P. *J. Phys. Chem. B* **2000**, *104*, 6499.
34. Schmidt, J. J.; Stafford, R. G. *FEBS Lett.* **2002**, *532*, 423.
35. Masuda, T.; Miiura, S.; Kano, N.; Sawa, N.; Japanese Patent (JP2184962), 1991.
36. Roothan, C. C. *J. Rev. Mod. Phys.* **1951**, *23*, 69.
37. Frisch, M. J.; Trucks, G. W.; Schlegel, H. B.; Scuseria, G. E.; Robb, M. A. Gaussian: Pittsburgh PA, 2003.
38. Hehre, W. J.; Radom, L.; Schleyer, P. V. R.; Pople, J. *Ab initio Molecular Orbital Theory*; Wiley: New York, 1986.
39. Pearlman, D. A.; Case, D. A.; Caldwell, J. W.; Ross, W. S.; Cheatham, T. E., III *Comput. Phys. Commun.* **1995**, *91*, 1.
40. Lacy, D. B.; Tepp, W.; Cohen, A. C.; Dasgupta, B. R.; Stevens, R. C. *Nat. Struct. Biol.* **1998**, *5*, 898.
41. Cieplak, P.; Cornell, W. D.; Bayly, C.; Kollman, P. A. *J. Comput. Chem.* **1995**, *16*, 1357.